Available online at www.sciencedirect.com
SCIENCE DIRECT®
Biochemical and Biophysical Research Communications 330 (2005) 1138–1145
BBRC
www.elsevier.com/locate/ybbrc

Genetic basis of phenotypic plasticity for predator-induced morphological defenses in anuran tadpole, *Rana pirica*, using cDNA subtraction and microarray analysis

Tsukasa Mori [a,*], Ikuei Hiraka [a], Youichi Kurata [a], Hiroko Kawachi [a], Osamu Kishida [b], Kinya Nishimura [b]

[a] *Laboratory of Marine Molecular Biochemistry, Department of Nihon University College of Bioresource Sciences, Kameino 1866, Fujisawa 252-8510, Japan*
[b] *Graduate School of Fisheries Sciences, Hokkaido University, Hakodate 041-8611, Japan*

Received 19 February 2005
Available online 23 March 2005

Abstract

Anuran tadpoles (*Rana pirica*) are induced to develop a higher tail and a bulgy body as predator-specific morphological responses when they are exposed to predatory larval salamanders. Subtractive hybridization was performed using induced tadpole body skin and normal tadpoles' body skin. A total of 196 clones showed higher expression, and 104 clones showed lower expression, when they formed bulgy bodies. In the subtraction, carboxypeptidase B, trypsinogen, elastase I, fibrinogen, elastase II, triacyl-glycerol lipase, and α1-antitrypsin genes showed lower expression. In contrast, RT-like protein, bullous pemphigoid antigen, phosphoserine aminotransferase, uromodulin, tetranectin, chaperonin-like protein, zinc finger protein, osteonectin, aldehyde dehydrogenase, Sec 23A protein, and ribosomal protein showed higher gene expression. Microarray analysis was also performed using this subtracted cDNA (nine replicates). Results of the microarray data essentially corresponded with those of the subtraction data, and the degree of the suppressed genes was much stronger than that of the expressed genes. Carboxypeptidase B showed the strongest suppression, and its inhibition range was from 1/100 to 3/100 compared with that of control body skin. Strong suppression was also observed with trypsinogen, elastase I, fibrinogen, and elastase II as well. These results can be interpreted as increases of fibrinolysis by strong depression of both carboxypeptidase B and other genes simultaneously, resulting in the retention of blood vessels and facilitating the circulation of blood. Expression was observed in phosphoserine aminotransferase, aldehyde dehydrogenase, RT-related protein, chaperonin-like protein, tetranectin, bullous pemphigoid antigen, uromodulin, and Sec 23A protein. They were significantly ($p < 0.05$) increased and were at least 1.5 times greater compared with the control. From the appearance, it seems that the bulgy shaped body is highly connecting to the bullous pemphigoid (BP) antigen that causes the skin blistering disorder, and tetranectin and uromodulin may be related to the extracell matrix through myogenesis, protein secretion, and ion transport, respectively. Since the RT-related protein gene derived from retrotransposon (L1) is known to disrupt mammalian transcriptomes, retrotransposon may be involved with phenotypic plasticity for morphological defense by *Rana prica* against predator threat.

Keywords: Phenotypic plasticity; cDNA subtraction; Microarray; Tadpole; Salamander; Bullous pemphigoid antigen; RT-related protein; Prey–predator interaction

Phenotypic plasticity is the ability of a single genotype to produce more than one alternative phenotype in response to environmental conditions [1]. Evolutionary biologists have demonstrated various examples of

* Corresponding author. Fax: +81 466 84 3805.
E-mail address: tellme07@brs.nihon-u.ac.jp (T. Mori).

0006-291X/$ - see front matter © 2005 Elsevier Inc. All rights reserved.
doi:10.1016/j.bbrc.2005.03.091

adaptive significance of phenotypic plasticity [2]. Organisms have various defensive systems in prey–predator interaction, such as escape and hide behaviors, chemical composition, and morphological changes against predators. Behavioral defenses and some of chemical composition in response to predator cues are adaptive phenotypic plasticity of organisms [3]. Morphological changes in response to predator cues have also been known in various aquatic organisms, such as cladocerans [4], bryozoans [5], ciliates [6], mayflies [7], snails [8], barnacles [9], amphibian larvae [10], and carp [11]. The precise mechanisms causing the morphological changes for this phenotypic plasticity due to prey–predator interaction might be different from the phenotypic plasticity of simply responding to abiotic environmental conditions. Since drastic morphological changes occurred in some tissues when prey–predator interaction had happened, signal transduction might have been involved with the developmental process. Despite that, in the last decade, molecular technologies have become accessible to the evolutionary ecologist, to address the ecology and evolution of complex phenotypes [12–14], researchers have still not reached the point of evaluating the genetic basis of phenotypic plasticity. In particular, there are no reports concerning the genetic background for phenotypic plasticity due to prey–predator interaction. Anuran tadpoles have been used as a model organism in studies of inducible phenotypes in evolutionary biology [15–18]. They exhibit inducible morphological changes in response to various types of predators. Among them, tadpoles of *Rana pirica* exhibit a striking inducible morphological defense [19].

Rana pirica, which is forest creature, usually spawns in small transient ponds formed by melting snow in early spring, in Hokkaido, Japan. The larvae of the species frequently cohabit with larval salamander, *Hynobius retardatus*. They form loose aggregations within parts of a pond. *H. retardatus* larvae prey on animals, including *R. pirica* tadpoles and conspecifics in the mixed school. In early spring, other predators have not yet emerged, and the two species interact closely [19]. Predation success depends on the gape size of the larval salamander and the body size of *R. pirica* tadpoles. Generally, *R. pirica* hatches earlier than *H. retardatus*, although the egg-laying periods overlap. Tadpoles and larval salamanders of various sizes coexist in a pond due to the random heterogeneity of the environment. Small tadpoles incur a size disadvantage in terms of predation threat. *R. pirica* tadpoles develop a bulgy body and a higher tail, using hypertrophic epithelial tissue (Fig. 1), when exposed to predation threat by their main predator larval salamander: *H. retardatus*. The bulgy morphology prevents *R. pirica* tadpoles from being swallowed by the larval salamanders [19]. Therefore, *R. pirica* tadpoles are considered to have evolved the inducible bulgy morphological against the gape-limited *H. retardatus* larvae under the intimate predator–prey relationship [19]. A preliminary histological investigation in the bulgy body of *R. pirica* tadpoles showed that epithelium makes up ca. 45% of the whole body volume, that the epithelium consists of fibroblasts and connective tissue, and it is saturated with lymph fluid (unpublished data).

In this paper, we address the genetic basis of the remarkable phenotypic plasticity, which attracts the attention of evolutionary ecologists. As the first step, we focused on the bulgy body skin tissue, which was the main part of the induced morphological change and the most downstream end of the gene interaction system for the phenotypic expression. Therefore, the molecular background in the typical tissue is very intriguing to ecologists. We investigated the differential transcriptome patterns using subtractive hybridization with bulgy body skin cDNA and normal tadpole body skin. Since a background clone is generally obtained by the subtractive hybridization system, the subtracted clone often does not reflect the real mRNA level.

Therefore, cDNA microarray analysis was also performed using these subtracted DNAs to confirm the results of subtraction, and further to identify what kinds of DNA were, and to what degree, expressed and repressed for phenotypic plasticity according to prey–predator interaction of tadpoles and salamanders. These two analyses clarified the gene expression pattern in the most downstream end of the gene regulation for phenotypic plasticity, which is a concern of evolutionary biologists.

Fig. 1. Induction of bulgy-bodied tadpole by presence of predatory larval salamanders. Control: basic morph in absence of the predators. Predator induced: bulgy morph induced by salamander.

Materials and methods

Induction of bulgy morph of tadpole R. pirica. We collected eggs of *R. pirica* and *H. retardatus* from some ponds in Hokkaido, Japan, from late May to early June in 2003. After hatching, *R. pirica* tadpoles were fed rabbit chow ad libitum. The larval *H. retardatus* was fed small size *R. pirica* tadpoles ad libitum. We designed an experiment to induce the predator-specific morphologies of *R. pirica* tadpoles. The experimental units were 4.5-L ($28.5 \times 16.5 \times 9.5$ cm) aquaria filled with 2 L of aged tap water. We randomly assigned 50 similarly sized, 10-day-old *R. pirica* hatchlings (mean ± SD, body length $= 8.62 \pm 1.32$ mm, $n = 30$) in each aquarium. We conducted the following two treatments which were replicated seven times to collect bulgy body skin and control body skin: (1) bulgy morph induction treatment—two salamander larvae in the aquarium (snout-vent length of the salamander larvae, mean ± SD, 17.80 ± 1.27 mm, $n = 20$), (2) non-induction treatment; without a predator in the aquarium. Induction of the bulgy morph requires close proximity to the larval salamander. The induction experiment was conducted in a laboratory at 16 °C and a natural LD regime. We exchanged water for all aquaria every 3 days throughout the experiment. Actual predation was minimized by replacing the larval salamander with others that were kept in holding tanks. After 10 days, we terminated the induction experiment and the tadpoles were used for RNA extraction.

RNA isolation from tadpoles. Only bulgy body skin and control body skin were collected by cutting it off with a razor from 50 to 80 tadpoles. These tissues were soaked into RNA later (Qiagen), respectively. These tissues were cut into small pieces with scissors and, after keeping them for 24 h at 4 °C, stored at −80 °C until experiments. Tissues were lysed and RNA was obtained using the Qiagen RNA mini preparation system according to the manufacturer's instruction. RNA yield was measured by absorbency at 260 nm and electrophoresis was performed.

Subtractive hybridization and TA cloning. cDNA synthesis and subtraction were performed using PCR-Select cDNA Subtraction Kits (Clontech) following the manufacturer's instruction. Since only a small amount of the total RNA was extracted from these tissues, the amount of the mRNA in the RNA (10 μg) was then pre-amplified using the SMART-PCR cDNA Synthesis Kit (Clontech). The mRNA from the bulgy body skin was used as a tester, and mRNA from the control body skin was used as a driver to obtain genes stimulated by the predator. Further, mRNA from control body skin was used as a tester, and mRNA from bulgy body skin was used as a driver to obtain suppressive genes due to the presence of the predator. Tester and driver cDNAs were separately digested with *Rsa*I. The *Rsa*I-digested tester cDNA was ligated with adapters and hybridized with an excess amount of *Rsa*I-digested driver cDNA to subtract the cDNA population which was present in both tester and driver. Residual single-stranded cDNA, rich in tester-specific cDNA population, was specifically amplified by PCR with primers corresponding to the adapters. Subtracted PCR products (4 μl) were mixed with pCRII-TOPO (Invitogen) solution (1 μl of diluted salt solution to 1/4 with DW, 1 μl vector) and incubated for 5 min at room temperature. The mixture (2 μl) was transferred to an electrocuvette containing 50 μl *Escherichia coli* (Top10) prepared for an electrocompetent, electrotransformation using Micro-Pulser (Bio-Rad) was performed. Transformed cells were cultured on LB agar plate supplemented with ampicillin (50 ppm), Xgal, and IPTG, and selected by blue-white selection. Single colonies were picked and screened for inserts using PCR. Randomly picked clones were sequenced for inserts using M13 Reverse or M13 (-20) Forward primers. DNA sequencing reaction was performed using BigDye Terminator v3.1/1.1 Cycle Sequencing kits (ABI), and sequencing samples were analyzed on ABI 3100DNA sequencer (ABI). Sequences were submitted for BLAST N and BLAST X analysis using public domain NCBI databases, and search homology through cDNA and protein was used. Annotation was decided through the use of a protein homology database using homologous sequences.

In the subtraction systems, generally fewer differentially expressed mRNAs and less quantitative difference in expression mean higher background even if obtaining a good enrichment of differentially expressed cDNAs. Therefore, differential screening step is usually performed to minimize background. In this experiment, however, we performed cDNA microarray analysis to obtain the real expression of these subtracted cDNA instead of differential screening.

cDNA microarray. Inserts in the pCRII-TOPO (Invitogen) were PCR amplified using primers from sequences flanking the cloning site. The PCR products (297) were purified by ethanol precipitation, and the PCR fragments were visualized on 0.8% agarose gel to ensure adequate PCR amplification prior to being robotically printed onto glass slides by DNA Chip Research Inc (Yokohama). PCR products were spotted onto the glass 9 replicates, and β-actin was used as a positive control and CHI, DFR, and λDNA were used as negative control genes. Total RNA (30 μg) extracted from each bulgy body skin and control body skin was dissolved in each 6 μl of 5× first strand buffer mixed with 10 pmol of mixed oligo(dt) primer (20mer), and DTT (10 mM), dNTPmix (3 mM dTTP, 2 mM aminoallyl-dUTP, 5 mM dATP, dGTP, and dCTP), RNase inhibitor, Super Script II (Invitrogen), and RNase-free water was added to a total volume of 20 μl. RT reaction was performed and incubated for 90 min at 42 °C. The reaction was terminated with 5 μl of 0.5 M EDTA (pH 8.0) and then incubated for 70 °C for 20 min after adding 10 μl NaOH for RNA degradation. The aminoallyl labeled cDNAs were purified by QIAquick PCR purification Kit (Qiagen) after neutralization with 10 μl of 1 N HCl. These cDNAs were precipitated with ethanol and then the pellets were dried and dissolved with 18 μl of (0.2 M $NaHCO_3$–Na_2CO_3: pH 9.0). Nine microliters of the aminoallyl labeled cDNAs was coupled with either Cy3 Mono-Reactive Dye Pack (Amersham Bioscience) or Cy5 Mono-Reactive Dye Pack (Amersham Bioscience) by adding 1 μl of diluted Cy3 or Cy5 with 45 μl DMSO. In the dark conditions, the reaction was performed at room temperature for 1 h, and these samples were mixed by vortexing every 15 min. Then, DW was added to these samples to 50 μl, and these samples were purified by using a Microbio spin column 30 (Bio-Rad). These labeled cDNA samples were treated for ethanol precipitation and dried pellets were obtained. These pellets were resuspended with 10 μl DW, and 0.6 μl of these samples was used for 1% gel electrophoresis, and the gel was scanned by Typhoon (Amersham Bioscience) to check Cy3 and Cy5 labeling efficiency. After checking cDNA labeling, these samples were used as cDNA probes for hybridization. A dye swap experimental design comparing the same samples but using adverse dyes in the two hybridizations was used to compensate for dye-specific labeling effects. Each of the Cy3 and Cy5 labeled cDNA (9.4 μl) solutions was mixed together and was supplemented with 10 μl of 20× SSC (3 M NaCl, 0.3 M $C_6H_5Na_3O_7{\cdot}2H_2O$), 1.2 μl of 10% SDS, and 8 μl of 20× Denhardt's (0.4% BSA, 0.4% Ficoll, and 0.4% polyvinylpyrrolidone) + 1% SDS solution. After this the hybridization solution was heated (95 °C) for 2 min and then incubated on ice. Two microliters of calf thymus DNA solution (Sigma) was added to the hybridization solution and incubated at 42 °C for 5 min. The pre-warmed hybridization solution was dropped onto DNA chips, and cover glass was placed onto the solution without forming bubbles. These DNA chips were set into ArrayIt Hybridization Casette (Telechem International) and hybridized at 65 °C for 18 h. After hybridization; DNA chips were soaked into 2× SSC–0.1% SDS solution at room temperature, and cover glasses were removed by gently rocking of the chips. DNA chips were washed by soaking the solution for 20 min and occasionally shaken gently. Then, these chips were soaked in a low stringency wash buffer (0.2× SSC–0.1% SDS solution) and (0.05× SSC–0.1% SDS solution), and performed in the same manner. Chips were then dried by centrifuge at 600 rpm for 2 min, and scanned using GenePix (InterMedical) and analyzed data according to the manuals. Data were eliminated

that the summative average signal intensity of Cy3 and Cy5 was under 1000 and data were not significant using Student's t test against control (significant line: $p = 0.05$), and global normalization was performed.

Result

Induction of the bulgy morphology

Anuran tadpoles, *R. pirica*, induce predator-specific morphological responses under exposure to a predator larval salamander (*H. retardatus*) [19]. They induce not only higher tails but also bulgy bodies in the presence of larval salamanders (Fig. 1). The tadpoles with this specific morphological adaptation survived better when exposed to the corresponding predation risk [19].

cDNA subtraction between the bulgy and normal control tadpoles

We collected only body skin tissue from both bulgy and control tadpoles, and performed subtractive hybridization with these samples. The subtractive cloning strategy generated 300 clones, and 196 clones were obtained as higher expression genes, and 104 clones were lower expression genes, when bulgy bodies were formed. For these 300 clones, only major known genes are presented in Fig. 2.

The number of randomly obtained genes with low expression (104 clones) was almost half compared with genes with high expression (196 clones). Therefore, the probability of appearance of genes with low expression might have been twice the present probability, if the number of randomly selected clones had been the same (Fig. 2). This inferred that the degree of genes with low expression was much stronger compared with high expression genes. The gene with lowest expression compared with control was carboxypeptidase B and it reached 22 clones/104 clones by subtractive hybridization. The numbers of obtained clones showing suppressive degree ranked in descending order were for carboxypeptidase B, trypsinogen, elastase I, fibrinogen, elastase II, triacyl glycerol lipase, and α1-antitrypsin. Although various genes were obtained as higher expression, most of them were between one and three colonies. However, five RT-like protein genes were obtained in these experiments. It is unknown if these genes were completely identical, because they were fragmentary. Therefore, these genes were described as reverse transcriptase-like protein in Fig. 2. Moreover, bullous pemphigoid antigen, phosphoserine-aminotransferase, uromodulin, tetranectin, chaperonin-like protein, zinc finger protein, osteonectin, aldehyde dehydrogenase, Sec 23A protein, and ribosomal protein were obtained as up-regulated genes.

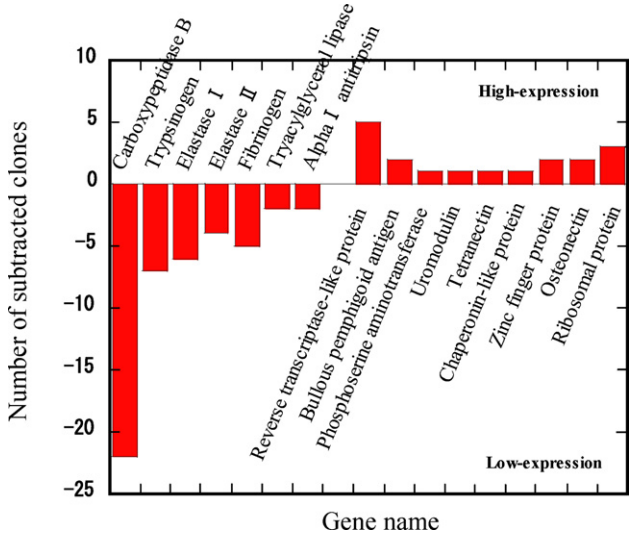

Fig. 2. Number of clones by subtracted hybridization using known genes. High-expression: the mRNA from the bulgy body skin was used as a tester and mRNA from the control body skin was used as a driver to obtain genes stimulated by the salamander. Low expression: the mRNA from the control body skin was used as a tester and mRNA from bulgy body skin was used as a driver to obtain suppressive genes due to the presence of the salamander.

DNA microarray analysis

We made microarray chips with ninth-replicated cDNA spots using subtracted cDNAs, and die swap analysis was performed (Figs. 3A and B). Data (120 spots) are plotted in Figs. 3A and B using data of statistical significance ($p < 0.05$) and genes capable of being annotated. Some major high and low expression genes are selected in Table 1. As we inferred from subtraction data (Fig. 2), carboxypeptidase B genes on the chips showed the greatest suppression of the gene expression in all clones, even though their cDNA lengths differed, as shown in Table 1. The suppression of carboxypeptidase B was in the range from 1/100 to 3/100 compared with that of control body skin. Strong suppression was also observed with trypsinogen, elastase I, fibrinogen, and elastase II as well. As we mentioned above, the subtracted numbers of clones were different. The tendency in these gene expressions obtained by the cDNA microarray mostly came close to corresponding with the data of subtraction.

Discussion

We obtained a list of transcriptions differentiating body morphology with and without exposure to predation risk (Table 1). This highlighted the first step in the whole mechanism of the bulgy morphological change. Even if there is a somewhat speculative deduction, at this step, it is important to deduce what is happening

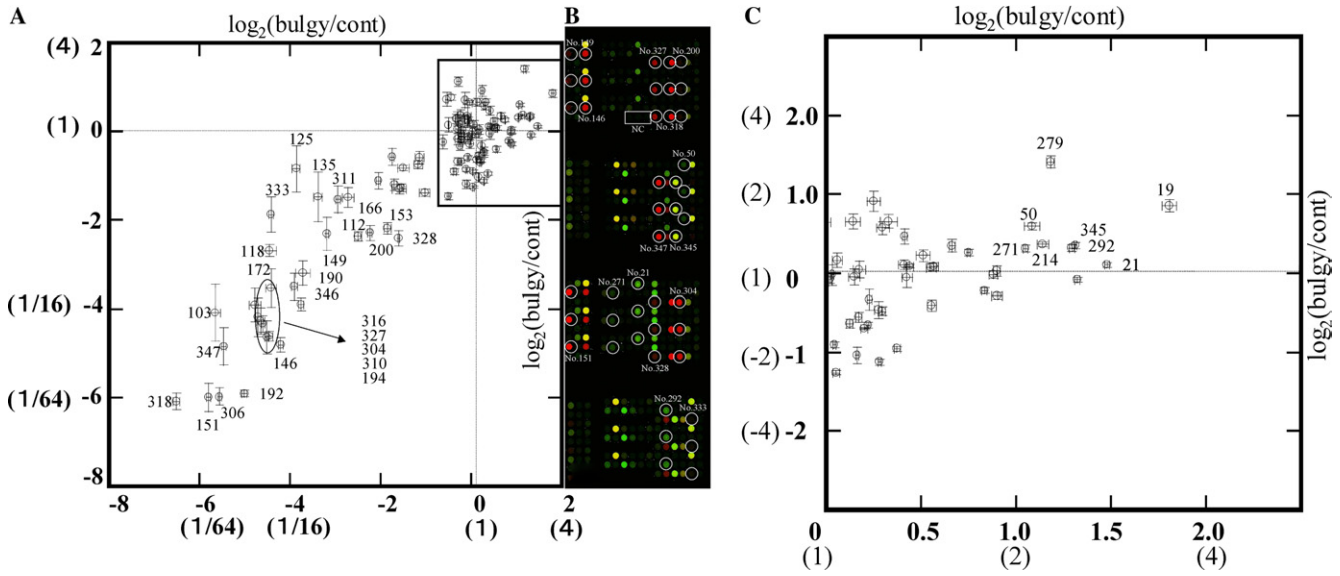

Fig. 3. The microarray analysis by the ratio of signal intensity using Cy3 and Cy5 derived from bulgy tadpole body skin and control tadpole body skin. These signals were performed by global normalization and are plotted on the graph using annotated genes. Values for increase or repression of genes expression against control are represented by $\log_2 X$–Y scales, and the numbers inside the parentheses show the values of integer rational number on a normal scale. The X axis indicates the ratios of bulgy body skin labeled with Cy5/control body skin labeled with Cy3. The Y axis is the ratios of bulgy body skin labeled with Cy3/control body skin labeled with Cy5. (A) Part of low expression. (B) Microarray hybridized with fluorescent labeled probes prepared from bulgy mRNA from body skin (Cy3) and control body skin (Cy5). Red indicates relatively higher expression in control body skin, which means repressed gene expression in bulgy body skin. Green indicates relative higher expression in bulgy body skin. Yellow indicates equal expression in both body skins. NC means negative control. (C) Part of up-regulation which is shown in boxed area in (A).

in the tissue, and what is required to generate the bulgy form when these tadpoles meet predator larval salamanders (Fig. 1). In the following, we make inferences about the functions of the genes with high and low expression in the bulgy tadpoles, referencing known functions in previous studies.

The list of genes repressed would be concerned in fibrinolysis. Carboxypeptidase B is well known to cleave off C-terminal lysine and arginine residues [20]. The C-terminal lysine residues of fibrinogen fragments are essential for binding of fibrinogen fragments to plasminogen [21], and plasminogen adsorbs in a sequential manner [22]. Molecular assembly of these proteins results in a ternary complex that efficiently generates plasmin on the surface of fibrin and thereby triggers the dissolution of a clot [23]. Therefore, removal of the C-terminal lysine and arginine residues attenuates the function of plasminogen activation, resulting in the prevention of accelerated plasmin formation and consequently downregulation of fibrinolysis [24]. Data of cDNA subtraction and microarray analysis (Figs. 2 and 3) showed strong depression of carboxypeptidase B and fibrinogen. These are indicative of up-regulation of fibrinolysis [25,26]. Furthermore, there is pro-carboxypeptidase B, which can be activated by proteolysis of the Arg-Ala peptide bond by trypsin or other Arg-specific serine proteinases [27]. Therefore, inhibition of trypsinogen is reasonable to keep a constant level of fibrinolysis (Figs. 2 and 3).

Elastase I and II, known as matrix metalloproteinase, also cleave fibrinogen and result in significantly impaired clotting [28], and at the same time, these enzymes degrade most of the constituents of the extracellular matrix, such as basement membrane, collagens, proteoglycans, fibronectin, and laminin [29]. Therefore, these enzymes become inactive by binding with α1-antitrypsin and α2-macroglobulin, respectively [30]. This α1-antitrypsin stimulates fibroblast proliferation and procollagen production. This implies that α1-antitrypsin may play a role in influencing tissue repair in vivo by directly stimulating fibroblast proliferation and extracellular matrix production via classical mitogen-activated signaling pathways [31]. This connective tissue formation at sites of tissue repair must be regulated by matrix protein synthesis and degradation, which in turn is controlled by the balance between proteases and antiproteases. Therefore, α1-antitrypsin might be decreased according to elastase I and elastase II as shown in Figs. 2 and 3.

The list of genes with high expression would be concerned in junctional adhesion. The bullous pemphigoid (BP) antigen, which is up-regulated in the bulgy tadpoles, was identified as a major autoantigen of the autoimmune skin blistering disorder bullous pemphigoid [32]. This BP antigen belongs to the plakin family of cytolinkers, and this is a cytoplasmic component of hemidesmosomes, which are junctional adhesion complexes in stratified and in complex epithelia [32]. Although a report indicated no related gene in chickens, frogs, and

Table 1
Identification of clones obtained by subtractive hybridization and microarray analysis

Sample ID	Chip 1 *Y* mean	Chip 2 *X* mean	Chip 1 *Y* SE	Chip 2 *X* SE	Fragment (bp)	Gene name	Mean(up or down)	Acc. No.	Homology % (protein)
Up									
19	0.856586	1.80799	0.078405	0.038086	582	Phosphoserine aminotransferase	2.52	AB182946	89
21	0.102988	1.47927	0.031347	0.011373	443	Aldehyde dehydrogenase	1.73	AB182947	93
50	0.593637	1.08352	0.045034	0.040533	583	Reverse transcriptase related protein	1.79	AB182948	57
214	0.366011	1.14058	0.028740	0.031392	640	Chaperonin-like protein	1.69	AB182949	96
271	0.308584	1.04915	0.040430	0.011363	118	Tetranectin	1.60	AB182950	81
279	1.407547	1.18219	0.076267	0.022521	416	Bullous pemphigoid antigen	2.45	AB182951	70
292	0.315859	1.29457	0.040802	0.014613	232	Uromodulin	1.75	AB182952	60
345	0.348434	1.31278	0.035923	0.006090	719	Sec 23A protein	1.78	AB182953	70
Down									
103	−4.082485	−5.64586	0.641384	0.114535	697	Carboxypeptidase B	0.03	AB182954	68
151	−5.995483	−5.80022	0.322221	0.046365	737	Carboxypeptidase B	0.02	AB182955	66
306	−5.975022	−5.55225	0.192823	0.042649	364	Carboxypeptidase B	0.02	AB182956	60
318	−6.083773	−6.50645	0.186513	0.069885	611	Carboxypeptidase B	0.01	AB182957	67
347	−4.848373	−5.45890	0.418733	0.047659	522	Carboxypeptidase B	0.03	AB182958	71
133	−3.895038	−3.75636	0.144852	0.061362	134	Elastase I	0.07	AB182959	70
153	−2.193203	−1.84403	0.131776	0.076264	312	Elastase I	0.25	AB182960	67
190	−3.192933	−3.71646	0.278726	0.164272	521	Elastase I	0.09	AB182961	72
200	−2.289094	−2.23716	0.171712	0.049107	132	Elastase I	0.21	AB182962	79
112	−2.364702	−2.49889	0.103427	0.086368	384	Elastase II	0.19	AB182963	60
146	−4.811679	−4.20999	0.162660	0.042729	402	Elastase II	0.04	AB182964	60
118	−2.689484	−4.45272	0.137863	0.153048	722	Fibrinogen	0.08	AB182965	96
125	−0.841810	−3.86459	0.517902	0.090656	427	Fibrinogen	0.20	AB182966	58
311	−1.540511	−2.93727	0.302717	0.046045	490	Fibrinogen	0.21	AB182967	96
333	−1.879239	−4.41737	0.401419	0.049666	591	Fibrinogen	0.11	AB182968	91
192	−5.905007	−5.00836	0.072883	0.060863	464	Trypsinogen	0.02	AB182969	60
310	−4.636817	−4.51474	0.372254	0.039350	426	Trypsinogen	0.04	AB182970	61
327	−4.268061	−4.64815	0.299183	0.086235	669	Trypsinogen	0.05	AB182971	57
304	−4.333330	−4.59732	0.181736	0.043604	455	Trypsinogen	0.05	AB182972	54
316	−4.180677	−4.70569	0.437786	0.052755	455	Trypsinogen	0.05	AB182973	52
346	−3.503325	−3.90045	0.304785	0.066941	433	Trypsinogen	0.08	AB182974	53
172	−3.530536	−4.42031	0.421806	0.118855	665	Alpha1 antitrypsin	0.06	AB182975	52
194	−4.611504	−4.46795	0.120925	0.085721	663	Alpha1 antitrypsin	0.04	AB182976	52
154	−3.905582	−4.77908	0.375894	0.124133	743	Alpha amylase	0.05	AB182977	70
166	−1.495047	−2.72252	0.222946	0.127695	667	Maltose glucoamylase	0.23	AB182978	45
135	−1.481054	−3.38251	0.560585	0.090594	248	Homo sapiens transmembrane protein UO-44D protein	0.19	AB182979	45
149	−2.309956	−3.18786	0.371917	0.032925	664	Triacylglycerol lipase	0.15	AB182980	74
328	−2.413999	−1.60291	0.174333	0.028887	770	Fructose-1,6-bisphosphatase	0.25	AB182981	77

The sample ID is derived from clone number. *X* and *Y* mean indicate averages of nine replicates of genes signal intensity by microarray calculated by global normalization, and SE represents standard err of replicates. Insert length is given in base pairs at fragment. Mean (up or down) indicates that these genes' expression is how many times greater or smaller than that of control based on the averages of 18 replicates of signal intensity. Percent homology is given by the protein database NCBI (BLAST X).

fish, by genomic Southern analysis using human BP 230 kDa antigen, the homology of our obtained gene showed a 230 kDa BP antigen [33] or similar to bullous pemphigoid antigen (230 kDa) (Table 1). This contradiction might be due to a difference in gene homology, because a high homologue ratio was obtained in protein data after translation. Considering the phenotypic type of tadpoles (Fig. 1), it seems very reasonable to express the BP antigen gene, and this creates the space between connective tissues that results in the bulgy form. The skin blistering disease in human beings is regarded as difficult to cure; therefore, mechanisms controlling phenotypic plasticity with this gene are very interesting, since the bulgy form returns to its original shape after a predator threat is removed [19].

Tetranectin is found in both serum and the extracellular matrix [34], and this works as progression of muscle differentiation [35]. Uromodurin, also known as Tamm–Horsfall protein, is a major glycoprotein synthesized in the mammalian pancreas and kidneys [36]. This is likely to play a critical role in intracellular assembly, regulated protein secretion, and ion transport [37,38].

We speculate that this uromodurin may serve to form a substrate for the bulgy body, and we have been analyzing fluid collected from the bulgy body by ESI-QTOFMS.

These data at first support fibrinolysis, and these blood vessels have to be normal, and further, controlling of connective tissues by the balance of degradation and enforcement is very important for the morphological change into the bulgy tadpole shape, as we speculated. RT-related gene (No 50) showed a greater increase compared with other RT-related genes. The RT-related protein gene was L1, and this was one of the retrotransposon members called long interspersed elements (LINEs). This is abundant in many eukaryotic genomes and contributes to genome structure and evolution by being autonomously mobilized by the copy and paste mechanism called retrotransposition [39]. A few studies indicated that retrotransposon has functional roles in the organisms that possess it [40,41]. It could be speculated that a certain functional mechanism of the RT-related protein genes would relate to induction of the bulgy body.

Acknowledgments

This work funded in part by the special subsidies for private school of Japan and Japanese grants from the Educational Ministry (16657071 and 16370008). Mori wishes to acknowledge my baby boy Akitoshi and my wife Miei for supporting my research life.

References

[1] M. Pigliucci, Phenotypic Plasticity, ed., The Johns Hopkins University Press, Maryland, 2001.
[2] C.D. Schlichting, M. Pigliucci, Phenotypic Evolution, ed., Sinauer Associates, Inc. Publishers, Sunderland, 1998.
[3] M.J. West-Eberhard, Developmental Plasticity and Evolution, ed., Oxford university press, Oxford, 2003.
[4] R. Tollrian, C.D. Harvell, The Ecology and Evolution of Inducible Defenses, ed., Princeton University Press, Princeton, 1999.
[5] C.D. Harvell, Predator-induced defenses in a marine bryozoan, Science 224 (1984) 1357–1459.
[6] J. Kusch, Induction of defensive morphological changes in ciliates, Oecologia 94 (1993) 571–575.
[7] J. Dahl, B.L. Peckarsky, Induced morphological defenses in the wild: predator effects on a mayfly, *Drunella coloradensis*, Ecology 83 (2002) 1620–1634.
[8] T.J. Dewitt, Costs and limits of phenotypic plasticity: tests with predator-induced morphology and life history in a freshwater snail, J. Evol. Biol. 11 (1998) 465–480.
[9] C.M. Lively, Predator-induced shell dimorphism in the acorn barnacle *Chthamalus anisopoma*, Evolution 40 (1986) 232–242.
[10] J. Van Buskirk, M. Arioli, Dosage response of an induced defense: how sensitive are tadpoles to predation risk? Ecology 83 (2002) 1580–1585.
[11] C. Bronmark, J.G. Miner, Predator-induced phenotypical change in body morphology in crucian carp, Science 258 (1992) 1348–1350.
[12] M. Pigliucci, Phenotypic integration: studying the ecology and evolution of complex phenotypes, Ecol. Lett. 6 (2003) 265–272.
[13] S.C. Stearns, P. Magwene, The naturalist in a world of genomics: an american society of naturalists symposium paper, Am. Nat. 161 (2003) 171–180.
[14] M.A. Thomas, R. Klaper, Genomics for the ecological toolbox, Trends Ecol. Evol. 19 (2004) 439–445.
[15] J. Van Buskirk, A comparative test of the adaptive plasticity hypothesis: relationships between habitat and phenotype in anuran larvae, Am. Nat. 160 (2002) 87–102.
[16] S.A. McCollum, J.D. Leimberger, Predator-induced morphological changes in an amphibian: predation by dragonflies affects tadpole shape and color, Oecologia 109 (1997) 615–621.
[17] A. Laurila, P.A. Crochet, J. Merila, Predation-induced effects on hatchling morphology in the common frog (*Rana temporaria*), Can. J. Zool. 79 (2001) 926–930.
[18] B. Lardner, Plasticity or fixed adaptive traits? Strategies for predation avoidance in *Rana arvalis* tadpoles, Oecologia 117 (1998) 119–126.
[19] O. Kishida, K. Nishimura, Bulgy tadpoles: inducible defense morph under the specific predator–prey system, Oecologia 140 (2004) 414–421.
[20] J.E. Folk, in: P.D. Boyer (Ed.), The Enzymes, Academic press, New York, 1971.
[21] M. Camacho, M.C. Fondaneche, P. Burtin, Limited proteolysis of tumor cells increases their plasmin-binding ability, FEBS Lett. 245 (1989) 21–24.
[22] B. Wiman, D. Collen, Molecular mechanism of physiological fibrinolysis, Nature 272 (1978) 549–550.
[23] E. Suenson, O. Lutzen, S. Thorsen, Initial plasmin-degradation of fibrin as the basis of a positive feed-back mechanism in fibrinolysis, Eur. J. Biochem. 140 (1984) 513–522.
[24] A. Redlitz, A.K. Tan, D.L. Eaton, E.F. Plow, Plasma carboxypeptidases as regulators of the plasminogen system, J. Clin. Invest. 96 (1995) 2534–2538.
[25] D.L. Eaton, B.E. Malloy, S.P. Tsai, W. Henzel, D. Drayna, Isolation, molecular cloning, and partial characterization of a novel carboxypeptidase B from human plasma, J. Biol. Chem. 266 (1991) 21833–21838.
[26] R.R. Hantgan, C.W. Francis, V.J. Marder, Basic Principles and Clinical Practice, ed., J.B. Lippincott, Philadelphia, PA, 1994.
[27] A.K. Tan, D.L. Eaton, Activation and characterization of procarboxypeptidase B from human plasma, Biochemistry 34 (1995) 5811–5816.
[28] O. Hiller, A. Lichte, A. Oberpichler, A. Kocourek, H. Tschesche, Matrix metalloproteinases collagenase-2, macrophage elastase, collagenase-3, and membrane type 1-matrix metalloproteinase impair clotting by degradation of fibrinogen and factor XII, J. Biol. Chem. 275 (2000) 33008–33013.
[29] J.F. Woessner Jr., Matrix metalloproteinases and their inhibitors in connective tissue remodeling, Faseb J. 5 (1991) 2145–2154.
[30] M.C. Geokas, J.W. Brodrick, J.H. Johnson, C. Largman, Pancreatic elastase in human serum. Determination by radioimmunoassay, J. Biol. Chem. 252 (1977) 61–67.
[31] K. Dabbagh, G.J. Laurent, A. Shock, P. Leoni, J. Papakrivopoulou, R.C. Chambers, Alpha-1-antitrypsin stimulates fibroblast proliferation and procollagen production and activates classical MAP kinase signalling pathways, J. Cell Physiol. 186 (2001) 73–81.
[32] J.R. Stanley, T. Tanaka, S. Mueller, V. Klaus-Kovtun, D. Roop, Isolation of complementary DNA for bullous pemphigoid antigen by use of patients' autoantibodies, J. Clin. Invest. 82 (1988) 1864–1870.

[33] M. Amagai, G.W. Elgart, V. Klaus-Kovtun, J.R. Stanley, Southern analysis of the 230-kDa bullous pemphigoid antigen gene in normal humans, animals, and patients with junctional epidermolysis bullosa, J. Invest. Dermatol. 97 (1991) 249–253.

[34] I. Clemmensen, L.C. Petersen, C. Kluft, Purification and characterization of a novel, oligomeric, plasminogen kringle 4 binding protein from human plasma: tetranectin, Eur. J. Biochem. 156 (1986) 327–333.

[35] U.M. Wewer, K. Iba, M.E. Durkin, F.C. Nielsen, F. Loechel, B.J. Gilpin, W. Kuang, E. Engvall, R. Albrechtsen, Tetranectin is a novel marker for myogenesis during embryonic development, muscle regeneration, and muscle cell differentiation in vitro, Dev. Biol. 200 (1998) 247–259.

[36] S. Fukuoka, S.D. Freedman, G.A. Scheele, A single gene encodes membrane-bound and free forms of GP-2, the major glycoprotein in pancreatic secretory (zymogen) granule membranes, Proc. Natl. Acad. Sci. USA 88 (1991) 2898–2902.

[37] V. Bazil, J.L. Strominger, Metalloprotease and serine protease are involved in cleavage of CD43, CD44, and CD16 from stimulated human granulocytes. Induction of cleavage of L-selectin via CD16, J. Immunol. 152 (1994) 1314–1322.

[38] P.C. Elwood, J.C. Deutsch, J.F. Kolhouse, The conversion of the human membrane-associated folate binding protein (folate receptor) to the soluble folate binding protein by a membrane-associated metalloprotease, J. Biol. Chem. 266 (1991) 2346–2353.

[39] M. Kajikawa, N. Okada, LINEs mobilize SINEs in the eel through a shared 3′ sequence, Cell 111 (2002) 433–444.

[40] M. Shimamura, M. Nikaido, K. Ohshima, N. Okada, A SINE that acquired a role in signal transduction during evolution, Mol. Biol. Evol. 15 (1998) 923–925.

[41] J.S. Han, S.T. Szak, J.D. Boeke, Transcriptional disruption by the L1 retrotransposon and implications for mammalian transcriptomes, Nature 429 (2004) 268–274.